Proc. Natl. Acad. Sci. USA
Vol. 96, pp. 1563–1568, February 1999
Medical Sciences

Mutation of *Pten/Mmac1* in mice causes neoplasia in multiple organ systems

KATRINA PODSYPANINA*, LORA HEDRICK ELLENSON†, ADRIANA NEMES‡, JIANGUO GU§, MASAHITO TAMURA§, KENNETH M. YAMADA§, CARLOS CORDON-CARDO¶, GIORGIO CATORETTI*, PETER E. FISHER*, AND RAMON PARSONS*‖

*Departments of Pathology and Medicine and ‡Howard Hughes Medical Institute and Center for Neurobiology and Behavior, College of Physicians and Surgeons, Columbia University, 630 W. 168th Street, P&S 14–453, New York, NY 10032; †Department of Pathology, Cornell University School of Medicine, 1300 York Avenue, New York, NY 10021; §Craniofacial Developmental Biology and Regeneration Branch, National Institute of Dental Research, National Institutes of Health, Building 30, Room 421, 30 Convent Drive MSC 4370, Bethesda, MD 20892-4370; ¶Department of Pathology, Memorial Sloan-Kettering Cancer Center, 1275 York Avenue, New York, NY 10021

Communicated by Bert Vogelstein, Johns Hopkins Oncology Center, Baltimore, MD, December 8, 1998 (received for review November 6, 1998)

ABSTRACT ***Pten/Mmac1*+/− heterozygous mice exhibited neoplasms in multiple organs including the endometrium, liver, prostate, gastrointestinal tract, thyroid, and thymus. Loss of the wild-type allele was detected in neoplasms of the thymus and liver. Surprisingly, tumors of the gastrointestinal epithelium developed in association with gut lymphoid tissue. Tumors of the endometrium, thyroid, prostate, and liver were not associated with lymphoid tissue and appeared to be highly mitotic. In addition, these mice have nonneoplastic hyperplasia of lymph nodes that was caused by an inherited defect in apoptosis detected in B cells and macrophages. Examination of peripheral lymphoid tissue including lymphoid aggregates associated with polyps revealed that the normal organization of B and T cells was disrupted in heterozygous animals. Taken together, these data suggest that PTEN is a regulator of apoptosis and proliferation that behaves as a "landscaper" tumor suppressor in the gut and a "gatekeeper" tumor suppressor in other organs.**

A search for a candidate suppressor of brain, prostate, and breast tumors led to the discovery of *PTEN/MMAC1/TEP1* (1–3). Analysis of various forms of human solid tumors suggests that *PTEN* is commonly inactivated during tumor evolution. Biallelic genetic alteration has been detected in 23–44% of glioblastomas, 35–50% of endometrial cancers, 35% of metastatic prostate cancers, 43% of malignant melanomas, and 4–6% of breast cancers (1, 2, 4–14). Mutation of *PTEN* appears to occur early in tumor development in endometrial cancer but late in the development of glial, prostate, and skin tumors. A broad survey of over 70 tumor cell lines originating from a variety of tissues identified that 30% had mutations on both alleles (6).

Mutations of *PTEN* have been documented in over 80% of kindreds with Cowden's disease (CD) (15, 16). CD is defined by the presence of cutaneous benign hamartomatous tumors, and the penetrance of intestinal polyposis appears to be approximately 70–85% (17–18). A subset of CD patients also develop thyroid and breast cancer. Inherited mutations of *PTEN* are also seen in most families with Bannayan–Zonana syndrome (19, 20). Individuals with this syndrome are affected in the first decade and have many intestinal polyps accompanied by enlarged heads and developmental delay. Germline frameshift, nonsense, and missense mutations cluster in exon 5, which contains the phosphatase domain.

Introduction of PTEN inhibits cell growth in many different cell lines (21, 22). Maehama and Dixon have shown that PTEN removes from phosphatidylinositol 3,4,5-triphosphate ($PIP_{3,4,5}$) a phosphate from the 3 position of the inositol ring (23). Moreover, mutated alleles identified from patient specimens that were expressed as protein and purified from bacteria are deficient for phospholipid phosphatase activity (24). One protein that is activated by $PIP_{3,4,5}$ is the antiapoptotic AKT. Recent evidence indicates that lack of PTEN in fibroblasts makes them resistant to several apoptotic stimuli (25). Tumor lines and fibroblasts that are null for PTEN have elevated levels of $PIP_{3,4,5}$ and active AKT when compared with matched cells expressing PTEN (24–26). Furthermore, introduction of PTEN into breast cancer cell lines induces apoptosis, which depends on an intact phosphatase domain and correlates with a down-regulation of AKT (22). Finally, dominantly active AKT is able to rescue cells from PTEN-mediated apoptosis (22, 25).

The coding sequence of the mouse homologue of *PTEN*, *Pten*, is identical to the human gene with the exception of a threonine to serine change at codon 400 (2). To develop a model of tumor progression in the mouse, we have introduced a deletion of PTEN into exon 5 that contains the phosphatase domain and is the most frequently mutated exon in the germline.

METHODS

Gene Targeting. A 129Sv/J genomic bacterial artificial chromosome (BAC) library (Research Genetics, Huntsville, AL) was screened with the human *PTEN* cDNA. The targeting vector was generated by ligating a 5′ arm (5.5-kb *Bgl*II-*Bgl*II fragment containing exon 4 and part of exon 5) and 3′ arm (2.7-kb *Bgl*II-*Eco*RI fragment) flanking a neomycin resistance cassette (1.7-kb *Xho*I-*Xho*I fragment of pPGK neo bpA) in the vector pZErO-2.1. Correct targeting in embryonic stem cells resulted in deletion of gene sequence from the *Bgl*II site in exon 5 to the next *Bgl*II site 2.0 kb downstream that was verified with flanking probes A and B. Loss of heterozygosity analysis made use of probe B on blots of tumor and normal tissue DNA. Genotyping postimplantation embryos was performed as described previously (27). Blastocysts were individually collected in PCR buffer.

Analysis of mRNA. Total RNA was extracted from liver. Randomly primed cDNA was prepared from each of the tissues studied. Reverse transcription–PCR (RT-PCR) reactions were performed with primer pair spanning the entire ORF. The truncated RT-PCR products were cycle sequenced (Amersham Pharmacia) for 22 cycles and resolved on 6% polyacrylamide gel to identify the mutant ORF. For Northern blotting analysis, a full-length human *PTEN* probe used and PTPH1 was excised from HFKAB49 (American Type Culture Collection) by using *Xba*I and *Hin*dIII. Both probes were labeled with [^{32}P]dCTP by using a primer II kit (Stratagene) and were used sequentially after

The publication costs of this article were defrayed in part by page charge payment. This article must therefore be hereby marked "*advertisement*" in accordance with 18 U.S.C. §1734 solely to indicate this fact.

PNAS is available online at www.pnas.org.

Abbreviations: CD, Cowden's disease; $PIP_{3,4,5}$, phosphatidylinositol-3,4,5-triphosphate; BAC, bacterial artificial chromosome; RT-PCR, reverse transcription—PCR; PI, propidium iodide.

‖To whom reprint requests should be addressed. e-mail: rep15@columbia.edu.

stripping and reprobing a blot containing mRNA from embryos of 7–17 days gestation (CLONTECH).

Detection of Intestinal Polyps. Mice were euthanized by CO_2 inhalation and perfused with PBS containing heparin followed by 10% buffered formalin. The gastrointestinal tract was dissected out from esophagus to anus and cut along the antimesenteric border.

Immunohistochemical and Flow Cytometric Analysis. Rabbit polyclonal antibody MT478 against PTEN was produced by immunization with 6-His-tagged recombinant PTEN expressed in *Escherichia coli* as described. IgG was purified from antisera using GammaBind G Sepharose (Amersham Pharmacia). Specificity of the anti-mouse Pten antibody (MT478) was established by using whole cell lysates in immunoblot analyses.

Paraffin-embedded sections from whole mouse embryos 8 to 16 days postcoitum (Novagen) were deparaffinized and rehydrated through xylene and ethanol into PBS. Endogenous peroxidase activity was quenched by incubation for 30 min in 0.3% H_2O_2 in methanol. After being washed twice with PBS, the sections were blocked with 5% goat serum plus 2% BSA for 30 min at 37°C and then were incubated with MT478 or preimmune serum overnight at 4°C by using 8 μg/ml IgG each. Immunohistochemical staining was performed according to the manufacturer's instructions with diaminobenzidine by using Vector Laboratories ABC kits. Immunohistochemistry on formalin-fixed paraffin-embedded adult tissue sections was performed essentially as published (28, 29) by using rat CD45R/B220 rabbit anti-CD3 (Dako), rat anti-Mac2 (kind gift of J. Thorbecke, New York University) (30), rabbit anti-Ki67 (gift of J. Gerdes, Molecular Immunology, Borstel, Germany), rabbit anti-vWF and mouse anti-desmin (Dako). Biotin-conjugated species-specific secondary antibodies were used, followed by Avidin-HRP (Dako). Double color immunohistochemistry was performed as published (29).

Single-cell suspensions of bone marrow, thymus, spleen, and lymph nodes were obtained from wild-type and Pten+/− mice after CO_2 euthanasia. After depletion of mature red blood cells by hypotonic lysis, cells were placed in ice-cold PBS supplemented with 10% heat-inactivated fetal calf serum and 0.1%NaN3 and kept on ice. The cells were stained with appropriate combinations of fluorochrome and/or biotin-labeled monoclonal antibodies (see below) (31), washed, and split into two sets. One set was washed once with Annexin V buffer (10 mM Hepes/NaOH, pH 7.4/140 mM NaCl/2.5 mM CaCl2) and incubated at room temperature for 15 min with 50 μl buffer containing 2.5 μl fluorescein isothiocyanate-conjugated recombinant Annexin V (PharMingen) and 5 μl propidium iodide (PI) (Sigma) (50 μg/ml), diluted to 400 μl with the same buffer and analyzed. Live (Annexin V negative, PI negative), early (Annexin V positive, PI negative) and late (Annexin V positive, PI positive) apoptotic cells were quantitated. The other set was fixed with a fluorescence-activated cell sorter lysing solution (Beckton-Dickinson) for 10 min, washed twice, blocked with 1% human type AB serum (Sigma), incubated overnight with a mouse anti-mouse Ki-67 (MIB 5; Immunotech, Westbrook, ME) or a control negative IgG1 monoclonal antibody and counterstained with a fluorescein isothiocyanate-conjugated rat anti-mouse IgG1 antibody (PharMingen). 30,000 lymphoid cells were analyzed on a five-color FACStar Plus flowcytometer (Beckton Dickinson) with PI exclusion of dead cells. Fluorochrome-conjugated antibodies for flow cytometry were: APC-or Pe-anti B220 (RA3–6B2), Pe- or biotin CD43 (S7), APC-, Pe- or biotin-Mac-1(M1/70), Pe-CD3 (2C11), APC-CD4, Pe-CD8, biotin-CD90 (Thy-1.2), APC-Avidin (PharMingen), Texas Red-conjugated goat anti-IgM, Pe-IgD (Southern Biotechnology Associates) and Texas Red-Avidin (Vector Laboratories).

RESULTS

Targeted Disruption of Pten in Mice. To identify the mouse homologue of human *PTEN,* a human cDNA clone was used to probe an arrayed library of mouse genomic BACs. Five clones were identified, two of which contained the entire *Pten* gene. Because the phosphatase domain, which is in exon 5, is frequently the target of missense and nonsense mutations in humans, we chose to target this domain for deletion (Fig. 1*a*).

A 10-kb fragment containing exons 4 and 5 from BAC 455G20 was subcloned into a plasmid vector. A portion of exon 5 containing the phosphatase domain was deleted and replaced with a neomycin resistance cassette in the same orientation as *Pten*. The construct was linearized and electroporated into W9.5 embryonic stem cells. Neomycin-resistant clones were screened by Southern blot for homologous recombination of the targeting construct. Of 144 clones tested for recombination, nine clones generated the expected 5-kb *Sac*I restriction fragment. Analysis of these clones digested with *Kpn*I and hybridized with a contralateral probe also gave the expected results (data not shown).

Two of the clones were selected for injection into C57BL6/J blastocysts and implanted in pseudopregnant females. Seven chimeras were generated from clone A and three from clone B. Multiple chimeras from each clone were capable of transmitting the mutation through the germline (Fig. 1*b*).

To determine the effect of the exon 5 mutation on *Pten* expression, cDNA was prepared from +/− and +/+ samples. Amplification of the +/+ cDNA with *Pten* primers resulted in the expected band of 1.2 kb, while amplification of the +/− cDNA with the same primers yielded two bands of 1.2 kb and approximately 1 kb (Fig. 1*c*). Sequence analysis of the truncated product revealed that exons 4 and 6 were spliced together, deleting all 239 bp of exon 5. The predicted protein product of this aberrant transcript is expected to contain the first 84 amino acids of Pten followed by 14 amino acids generated by the frame shift.

Pten Is Essential for Embryonic Development. Heterozygous mice were crossed against each other and no viable −/− progeny were detected of 54 offspring ($P < 0.005$, χ^2) (Table 1). To determine when development was arrested in the −/− mice, we

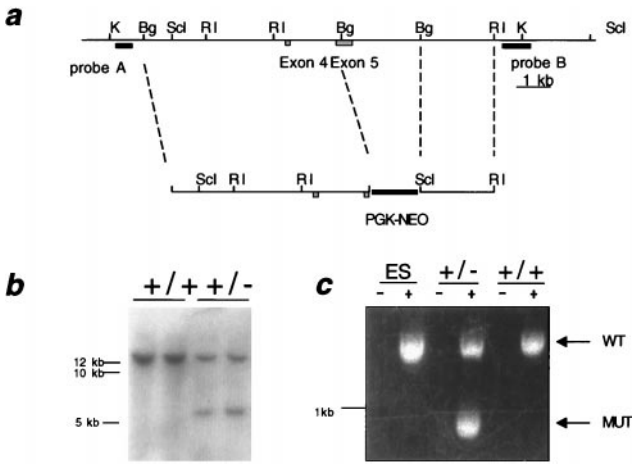

FIG. 1. Targeted disruption of Pten in mice. (*a*) Restriction map of Pten and the targeting construct. Restriction sites are as follows: *Kpn*I (K), *Bgl*II (Bg), *Sac*I (ScI), *Eco*RI (RI). The targeting construct contains a cassette of the phosphoglycerate kinase promoter upstream of the neomycin resistance gene ORF (PGK-NEO), which has replaced the *Bgl*II fragment containing the phosphatase domain in exon 5. (*b*) Southern blot of mouse tail DNA digested with *Sac*I and hybridized with probe B. The samples loaded are the offspring of a chimera × C57BL6 mating. The two lanes on the left have only the wild-type band while the two lanes on the right have both the wild-type and mutant bands. (*c*) RT-PCR analysis of Pten. RNA was prepared from W9.5 embryonic stem cells and the livers of +/+ and +/− littermates. RNAs were either reverse transcribed (+) or placed in mock reactions (−), and the entire ORF was amplified with a single pair of primers. After electrophoresis on a 1% agarose gel and staining with ethidium bromide, the expected wild-type 1.2-kb band was detected in all samples subjected to reverse transcription. The sample from the +/− mouse also produced a product just under 1 kb.

Table 1. Genotypic analysis of Pten-mutant matings

Matings (M × F)	Strain	Day of analysis	Genotype +/+	+/−	−/−
+/− × +/+	B6/129 × B6/129	Newborn	58	61	0
+/− × +/−	B6/129 × B6/129	Newborn	16	38	0
		3.5	2	6	4
		6.5	4	7*	3†
		9.5	9	11	0
		15.5	4	4	0

*Two of these embryos were partially resorbed.
†All of these embryos were partially resorbed.

examined embryos at different days of gestation. Although no morphologically intact −/− embryos were found 6.5, 9.5, and 15.5 days postcoitum, four normal-appearing −/− blastocysts were observed at 3.5 days postcoitum. Our method of genotyping the 3.5- and 6.5-day postcoitum embryos relied on the use of microsatellites that were reportedly linked to *Pten* (32). To establish that *D19Mit88* was indeed close to *Pten*, 174 mice previously genotyped by Southern blotting were analyzed. From these mice, only two recombination events were detected indicating a genetic distance of 1–2 cM between *Pten* and *D19Mit88*. Thus the likelihood that all four embryos represented recombination events is less than $(0.02)^4 = 1.6 \times 10^{-7}$. Aberrant embryos were detected at day 6.5. These embryos appeared disorganized and were apparently undergoing a process of resorption. Their genotype indicated that the cells were primarily −/−. Thus, lethality appeared to occur after implantation but prior to gestation.

Expression of Pten Protein During Embryonic Development. Immunohistochemical analysis of mouse embryos (day 8 to day 16 postcoitum) revealed embryonic expression of Pten. As shown in Fig. 2, embryos at days 8, 9, and 10 express little but detectable Pten protein relative to the placenta. Expression became more pronounced by day 11. Similar or slightly higher levels of immunohistochemical staining for Pten were found in embryos at days 13–16, with prominent expression detected in the dorsal portion of the mantle layer of spinal cord, heart, and epidermis, but with general expression in a variety of tissues. Preimmune serum and anti-Pten serum incubated with purified Pten did not stain mouse tissues. The expression pattern was consistent with the results of Northern blot analysis. *Pten* mRNA expression of a 6.5-kb transcript was low on day 7 and was expressed at higher levels on day 11, 15, and 17 embryos. In contrast, the level of the 2.5-kB transcript of Pten was constant and the transcript of PTPH1 was highest on day 7 and plateaued on day 11 (data not shown).

Pten Heterozygotes and Neoplasia of Multiple Organs. Serial sections of the testes, prostate, brain, and thyroid were examined for 20 heterozygotes and four control littermates at a young age (ages 6–22 weeks, average 12.1 weeks). Follicular or papillary noninvasive neoplasia of the thyroid was found in three of the 20 mice (Fig. 3*a*). An additional three mice had atypical epithelial changes in the thyroid. Prostatic intraepithelial neoplasia was detected in three of the eight males and was seen in a setting of hyperplasia (Fig. 3 *d–f*). An additional three mice had foci of benign epithelial hyperplasia in the prostate. No brain or testicular lesions were found. To examine whether the cell cycle was disturbed in these lesions, we performed immunohistochemistry by using the antibody for Ki-67, which detects cells that are in G1, S, G2, or M but not G0 phase. Increased levels of staining were noted in the neoplastic epithelium of the thyroid and the hyperplastic epithelium of the prostate (Fig. 3 *b* and *e*). Stained cells detected positive mitoses at a distance from the basement membrane. Only occasional staining was detected in wild-type control tissue. Analysis of 129SvJ/C57B6 chimeras revealed the presence of prostatic and thyroid abnormalities as well.

We observed consistent changes in the endometrium (Fig. 3 *g–i*). One hundred percent (20/20) of heterozygous females of

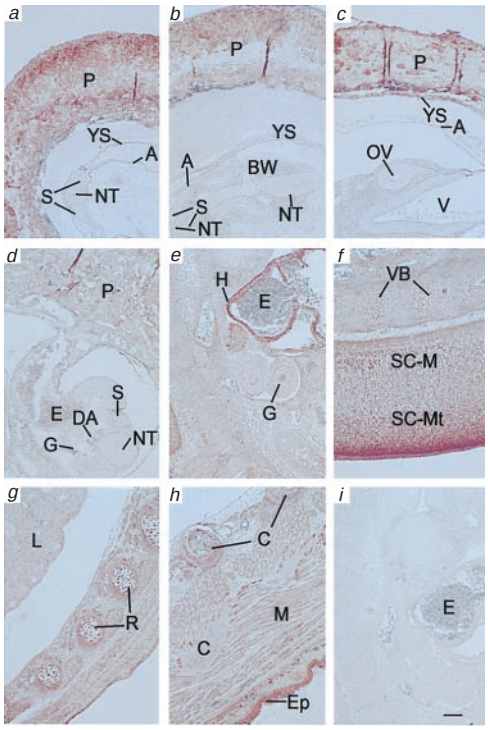

FIG. 2. Immunohistochemical protein expression patterns of PTEN in developing mouse embryos: day 8 (*a, b*), day 9 (*c*), day 10 (*d*), day 11 (*e*), day 13 (*f*), day 14 (*g*), and day 16 (*h*). In embryos from day 8 through approximately day 10, PTEN expression was minimal in tissues such as yolk sac (YS), neural tube (NT), somite (S), amnion (A), body wall (BW), optic vesicle (OV), and embryonic gut (G), yet was routinely positive in placenta (P) (*a–d*). From day 11, embryos expressed PTEN widely at moderate levels, including in lung (L), muscle (M), cartilage (C), vertebral body (VB), rib cartilage primordium (R), and marginal layer of the spinal cord (SC-M); enhanced expression was observed in heart (H), dorsal mantle layer of the spinal cord (SC-Mt), and epidermis (Ep). *i* was a day 11 embryo section stained with preimmune serum. Erythrocytes (E) displayed little or no staining at any stage. Other structures were brain ventricle (V) and dorsal aorta (DA). Scale bar = 1 mm.

which two were pregnant had multifocal endometrial complex atypical hyperplasia, a lesion thought to be the precursor of endometrial carcinoma in humans (age ranging from 18 to 39 weeks; mean 26.8 weeks). The uteri of wild-type littermates showed diffuse simple hyperplasia in three cases (3/12) and a single focus of complex atypical hyperplasia in one 33-week-old case (1/12) (age ranging from 7–48 weeks; mean 27.5 weeks).

In a group of older mice ranging in age from 20–56 weeks, 12% (30/256) of heterozygous mice died or were sacrificed because of morbidity (Fig. 3*j*). During this period, only one wild-type littermate (1/231) perished for unknown cause. Lymphomas developed in 7/256 +/− animals that were clinically sick and presented with thymic enlargement (5/7), splenomegaly (7/7), and diffuse microscopic infiltration of all organs by atypical immature lymphoid cells (7/7) (Fig. 3*c*). These lymphomas were lymphoblastic by histology, with high mitotic rate and occasional starry sky pattern. They were positive for cytoplasmic CD3 and negative for the B cell marker B220 ($n = 3$). All were examined for loss of heterozygosity of the wild-type allele by Southern blot, which was detected in 5/7 tumors (Fig. 3*k*).

Other tumors causing morbidity in +/− mice were found as well. One mouse developed synchronous thyroid carcinoma, liver adenoma, and poorly differentiated leukemia. Three mice developed bowel obstructions because of large adenomas of the colon. Infarction of the uterus was found in three mice, with one uterus containing a teratoma. Finally, two mice died because of diffuse

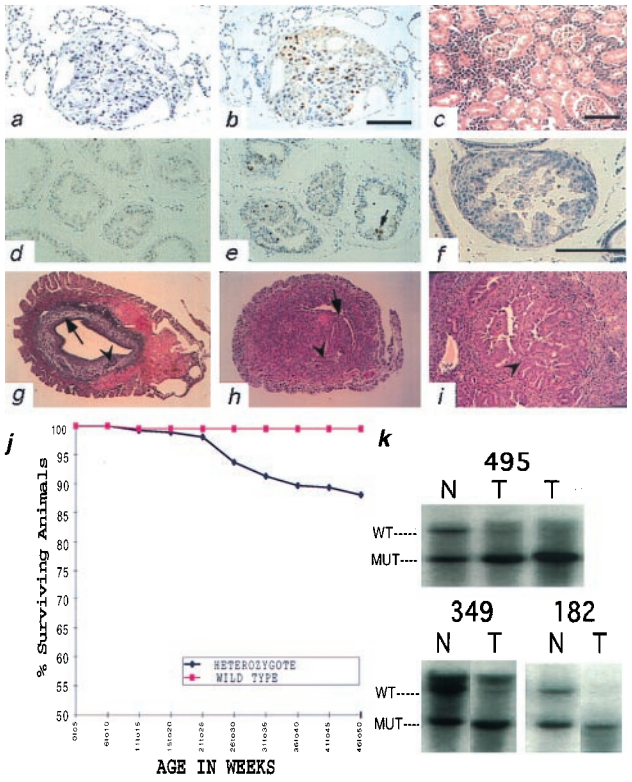

FIG. 3. Histological survey of tissues in Pten+/− mice. (*a*) Papillary thyroid carcinoma of 18-week-old Pten+/− male, hematoxylin/eosin (×400). (*b*) Anti-Ki67 stain of the same thyroid carcinoma. (*c*) A malignant lymphoma of the kidney of six-month-old Pten+/− male (case 87), hematoxylin/eosin (×200). (*d* and *e*) Immunohistochemical analysis of proliferation using anti-Ki67 antibody on prostates of +/+ (*d*) and +/− (*e*) mice. Arrow points to mitotic figure (×200). (*f*) Prostatic intraepithelial neoplasia found in 17-week-old Pten+/− male, hematoxylin/eosin (×400). (*g–i*) Mouse uteri. (*g*) Cross-section of the uterus of the 26-week-old wild-type mouse. Arrow points to the endometrium. Arrowhead points to the normal gland (×40). (*h*) Cross-section of the uterus of the 31-week-old heterozygous mouse. Arrow points to the endometrium. Arrowhead points to the atypical hyperplastic gland (×40). (*i*) Arrowhead points to a region of complex atypical hyperplasia in a 29-week-old heterozygous mouse (×100). (*j*) Decreased survival of the Pten heterozygous animals. (*k*) Loss of heterozygosity of Pten in tumors. Southern blots of normal-tumor pairs of three independent T-cell lymphomas analyzed with probe B. DNA was digested with *Sac*I.

lymph node hyperplasia of the neck and axilla that compressed major vessels.

Pten+/− Mice Are Predisposed to Intestinal Polyposis. During the examination of the alimentary tract, we noticed that multiple polyps were present in the large and small intestines of eight of nine chimeric mice (Fig. 4 *a* and *b*). The modal number of polyps per mouse was six and the range was 0 to 44. The polyps appeared to frequently cluster together. For example, in three chimeras multiple polyps were found within the caecum within a radius of less than a centimeter. In addition, another chimera had over 40 polyps limited to a 5-cm segment of its jejunum. The size of the polyps varied considerably, ranging from <1–6 millimeters. The only other masses of note were bilateral teratomas of the testicles in one mouse.

We next examined 17 heterozygotes at ages ranging from 7 to 18 weeks for the presence of polyps, which were found in all animals. These polyps were fewer in number and tended to be smaller. All mice had at least one polyp with a range of 1 to 15 and a mode of 2. As seen with the chimeras, multiple polyps frequently clustered within a single region. In parallel, we also examined seven wild-type *Pten*+/+ littermates and one

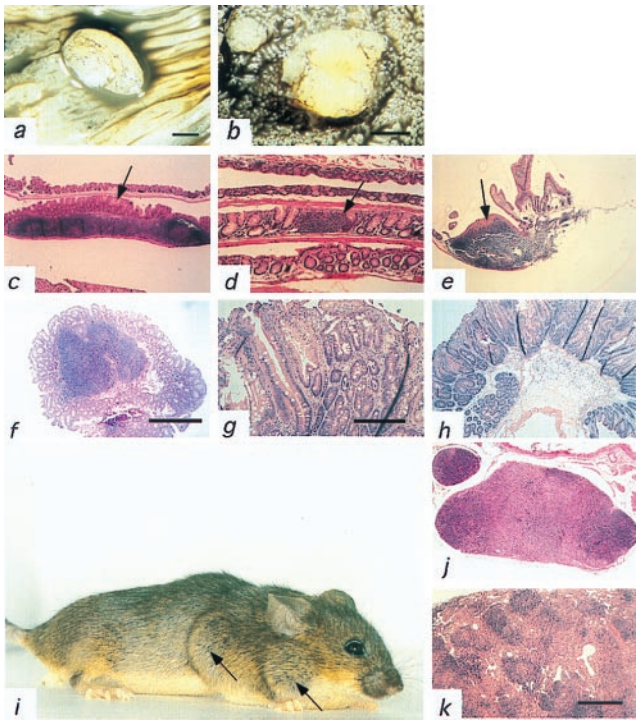

FIG. 4. Gross and histological appearance of gut polyps and lymphoid hyperplasia. (*a* and *b*) The gastrointestinal tract was cut longitudinally along the antimesenteric border and cleaned. Polyps were visualized by eye and then inspected with a dissecting microscope. Contrast was enhanced with india ink. (*a*) A 5-mm polyp (×6) at the colorectal boundary. (*b*) Two polyps in the jejunum of diameters of 2.5 and <1 mm (×20). (*c–e*) Clean mouse intestines were rolled and embedded in paraffin, sectioned, and stained with hematoxylin and eosin. Arrow indicates luminal side of the lymphoid aggregate. (*c*) Lymphoid aggregate in the colon of the wild-type mouse (×100). (*d*) Lymphoid aggregate in the small intestine of the wild type (×40). (*e*) Lymphoid aggregate in the small intestine of the heterozygous mouse (×100). Note association of polyp growth with the Peyer's patch. (*f*) A pedunculated polyp of the colon with hyperplasia and a lymphoid aggregate in the center (×40). (*g*) Hyperplastic polyp of the jejunum (×100). (*h*) Retention polyp of the colon (×40). (*i*) Pten+/− female with lymphadenopathy of neck and axilla (arrows). (*j* and *k*) Paraffin sections of (*j*) paracortical and medullary effacement and (*k*) paracortical effacement and follicular hyperplasia of the heterozygous mice (×40).

C57BL6/J male. All of the mice were examined as above for evidence of gross alterations, and no polyps were found.

Histologic Analysis of Gastrointestinal Polyps. To better understand the nature of the polyps, paraffin sections from 47 polyps were stained by hematoxylin and eosin (Fig. 4 *e–h*). A variety of morphologies was observed (Table 2). Most were classified as lymphoid polyps with normal-appearing epithelium overlaying a nodular aggregate of lymphoid cells with the location of the aggregate being the only abnormal feature. The second most frequent type, classified as lymphoid polyps with epithelial

Table 2. Histological types of the polyps in *Pten*+/−

Polyp type	Number observed
Lymphoid	23
Mixed lymphoid–hyperplastic	12
Mixed lymphoid–inflammatory	1
Mixed lymphoid–dysplastic	4
Mixed dysplastic–inflammatory	2
Hyperplastic	1
Dysplastic	2
Retention/Juvenile	2
Total	47

hyperplasia, was similar in morphology with the exception of the epithelium, which was hyperplastic. Two more polyps were classified as retention or juvenile polyps. In addition, a total of five polyps had elements of epithelial dysplasia, which indicates a potential for progression to a carcinoma. Normal lymphoid aggregates of the intestines of wild-type mice were associated with regions of flattened epithelium and crypts (Fig. 4 *c* and *d*).

Lymph Node Hyperplasia. Beginning at 20 weeks of age, we noticed large nodal masses in the neck and axilla of the heterozygous mice (Fig. 4*i*). By 50 weeks of age, all of the female mice and 45% of the male mice had similar lesions (Fig. 5*a*). These masses reached morbid size in some of the animals, and they were sacrificed. Histological analysis revealed multiple macroscopically enlarged lymph nodes and diffuse microscopical alterations of nonenlarged lymph nodes (submandibular> cervical > axillary > mesenteric) and splenomegaly (Fig. 4 *j* and *k*). Morphologic, immunohistologic, and flow cytometric analysis showed expansion of the interfollicular areas and medullary cords and residual follicular and paracortical hyperplasia composed of B, T, macrophage, and fibroblast cells with no evidence of clonal expansion. Abnormal lymphoid aggregates were also occasionally noted in the kidney and lung.

To determine whether the abnormal accumulation of cells of different lineages could be due to an inherited defect in proliferation, we compared healthy 4-week-old +/− and +/+ littermates. Cells of the thymus, lymph nodes, spleen, and bone marrow were collected. A cell cycle-specific antibody, Ki-67, was used in combination with antibodies to lineage-specific markers (B220, CD4, CD8, Mac1, CD90, CD43, μ, δ). No difference between the control and heterozygous population was observed in terms of lineage differentiation and proliferation (Fig. 5*c*). The same series of markers was used in conjunction with Annexin V to measure steady-state levels of apoptosis (Fig. 5*b*). Levels of Annexin V positive cells were generally lower in heterozygous B cells and macrophages. Differences in Annexin V binding were most significant in the bone marrow ($P < 0.05$; $P < 0.01$). These data suggest that +/− mice have a deficiency in B cell and macrophage apoptosis. No difference in Annexin V binding was seen in T cell populations, which was consistent with the observation that thymus weight and microscopic morphology were indistinguishable between +/+ and +/− animals (not shown).

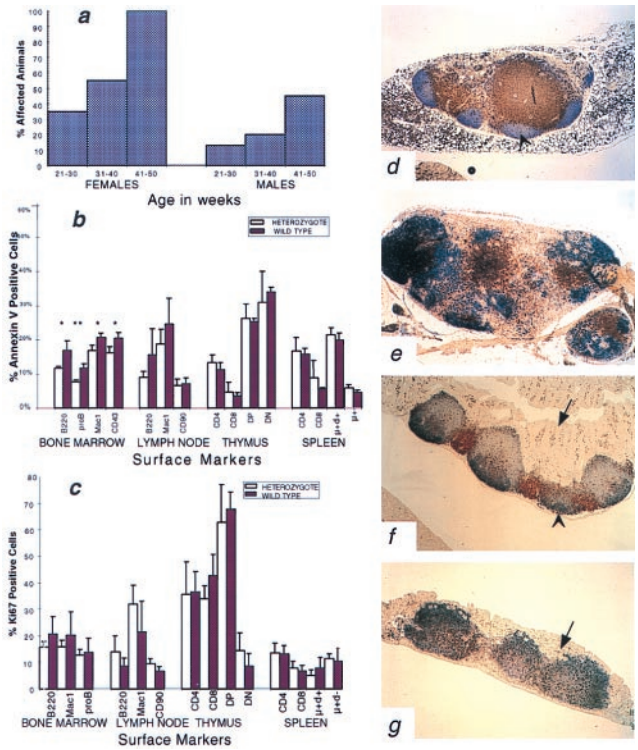

FIG. 5. Analysis of lymphoid abnormalities in Pten heterozygous mice. (*a*) Penetrance of the lymph node hyperplasia in different age and sex groups of Pten+/− mice (82 females, 86 males studied). (*b* and *c*) Flow cytometric analysis of cells from four lymphoid organs. Cells from three wild-type and three heterozygous animals labeled with various surface markers as indicated on the horizontal axis and then labeled with either annexin V antibody (*b*) or Ki67 antibody (*c*). One asterisk indicates $P < 0.05$, two asterisks indicate $P < 0.01$. (*d–g*) Immunohistochemical analysis of lymph nodes and lymphoid aggregates of the gut of the wild-type and heterozygous animals. CD3-positive cells appear brown and B220-positive cells appear blue. Arrows point to the lumen side of the intestinal wall. Arrowheads point to the germinal centers. (*d* and *e*) Lymph node of the wild-type (*d*) and heterozygous (*e*) mouse. (*f* and *g*) Colonic lymphoid aggregates of the wild-type (*f*) and heterozygous (*g*) mice.

Abnormalities of Lymphoid Tissue Architecture. The repeated observation of lymph node hyperplasia and lymphoid polyps led us to examine *in situ* the immune architecture of lymphoid tissue. Wild-type and heterozygous nodes and aggregates were stained for the T cell marker CD3 and the B cell marker B220. As expected, discrete B cell and T cell zones were found in the wild-type nodes and gut aggregates (Fig. 5 *d* and *f*). On the other hand, the staining pattern seen in +/− animals was quite different. In the hyperplastic lymph nodes and aggregates, follicular organization was blurred with mixing of the B and T cell regions (Fig. 5 *e* and *g*). This mixing was accompanied by erosion of the follicles by Mac-2+ macrophages and desmin+ fibroblasts, invasion of the germinal centers by T (CD3) lymphocytes, and fragmentation of germinal centers. This process involved to various extents all lymphoid tissues, including lymphoid aggregates associated with polyps. No evidence of a proliferative abnormality could be detected in the hyperplastic nodes (Ki-67).

DISCUSSION

The heterozygous mutation of Pten predisposes mice to a variety of different tumors. Lymphomas, dysplastic intestinal polyps, endometrial complex atypical hyperplasia, prostatic intraepithelial neoplasia, and thyroid neoplasms were each identified at least twice. Moreover, consistent with the model that *Pten* is a tumor suppressor, loss of the wild-type allele was frequently observed in mouse lymphomas. In humans, mutations of *PTEN* are found in all of these neoplasias. These data suggest that PTEN+/− mice will be a useful model system for the study of endometrial, prostate, and thyroid cancer.

Some human cancers associated with *PTEN* mutations, including neoplasia of the skin, breast, and brain are notably absent from the mice. Another discrepancy between germ-line mutations of *PTEN* in humans and mice is that we observed no clear examples of hamartomas. For instance, the tumors of the intestine did not exhibit any evidence of abnormalities of the organization of muscle or neural cells that are typically found in human gut hamartomas with *PTEN* mutations. Tumors of many tissues (lymphoma, thyroid, prostate, endometrium) were solely composed of a single cell type. Furthermore, in all tumor-bearing organ sites the mice seem to be predisposed to the development of malignant-appearing cells with evidence of dysplasia, a high mitotic index, and cell proliferation (Ki-67). In the case of the epithelial tumors, the cytologic hallmarks of carcinoma were detected frequently, but invasion of the basement membrane was rarely noted.

A startling phenotype is the lymphadenopathy because of lymph node hyperplasia seen in female and male heterozygotes. Based on the results of Annexin V binding, we propose that the Pten+/− mice have an inherited deficit in the apoptosis of constituent cells of the lymph node. This defect leads to the gradual accumulation of cells that have undergone insufficient selection and are therefore unable to maintain lymphoid architecture. The phenotype is strongly affected by the sex of the mouse, which may reflect sexual differences in the regulation of Pten or apoptosis. Whether Pten+/− mice have compromised immune function remains to be tested.

The aberrations of the immune system that have been observed in Pten+/− mice are reminiscent of phenotypes seen in mice that are deficient for Fas signaling. The *lpr/lpr* (a Fas mutant allele) and Fas−/− mice have lymphadenopathy and splenomegaly but normal development of thymocytes (33). Given the deficit in apoptosis that we have observed in B cells and macrophages and the observation that Pten−/− fibroblasts are resistant to apoptotic stimuli, it is possible that the hyperplasia may be the result of a deficit in Fas signaling (25).

Tumors of the intestine appear to exhibit a consistent pattern of development that differs substantially from the development of intestinal tumors in *Apc*+/− and *Smad2*−/− mice (34, 35). The smallest, earliest, and most frequent polyps detected in the Pten+/− mice were pedunculated or flat but always associated with a lymphoid aggregate. Lymphoid aggregates are a normal feature of the colon and small intestine, which are located in the interstitial space between the epithelium and muscularis propria and induce a specialized epithelium, in which the crypts or villi are flattened, for the presentation of antigen to lymphoid nodules (36, 37). Particularly large aggregates are found in the normal small intestine and are known as Peyer's patches. In Pten+/− mice, the lymphoid aggregates display abnormalities in the distribution of B and T cells. We propose that the most likely explanation for the development of tumors at these sites is that the abnormal aggregates are sending improper signals to the overlying epithelium inducing it to grow. Alternatively, the simple lymphoid polyps may create an environment prone to mechanical injury that is a nidus for hyperproliferation. Both of these models are consistent with the notion that *Pten* behaves as a "landscaper" in the colon (38). In fact, the principle of inflammatory cells establishing an environment for epithelial neoplasia in the colon has precedent in ulcerative colitis and Crohn's disease. Another possibility is that the epithelium itself induces the formation of the lymphoid aggregate. This possibility seems unlikely. Disturbances of immunologic homeostasis occur throughout the mouse; no increase in the number of aggregates was found in the colon, and the lymphoid organization of B and T cells is abnormal. All of these data suggest that the lymphoid tissue in the gut is unable to create a normal lymphoid nodule, which in turn leads to epithelial transformation.

The results presented in this paper differ to some extent from the results of Pten+/− mice reported by others (39, 40). The lethality in our mice occurs by 6.5 days, whereas it occurs later in the other mice. In addition, Di Cristofano *et al*. have seen frequent alterations of the skin and testes that have not been observed in our hands. On the other hand, the lymph node hyperplasia and the complex atypical hyperplasia of the uterus have not been reported by others. Furthermore, the other groups did not observe the close relationship between lymphoid aggregates and tumors of the intestine. The discrepancies of these papers may be due to differences in genetic background. An alternative explanation is that each group has engineered a unique mutation, each of which may be displaying varying hypomorphic or dominant-negative properties. Finally, the lymphoid hyperplasia that we have detected may reflect an abnormal response to an unidentified pathogen that is unique to our colony, although no viral, bacterial, or parasitic agent is detected by routine surveillance.

The data demonstrated in this paper suggest that Pten is a potent tumor suppressor in mice and humans. Furthermore, the mechanism of tumor suppression may function at the level of the cell in certain tissues and the organ microenvironment in others.

We thank N. Papadopoulos, Jing Li, Steven I. Wang, P. P. Pandolfi, A. Di Cristofano, M. Rubin, T. Ludwig, M. Peacocke, and C. Eng for their helpful discussions; E. Kandel for the BAC library; and R. Axel for embryonic stem cells and their maintenance. This work was supported by grants from the National Cancer Institute and the James S. McDonnell Foundation. G.C. is a Leukemia Society of America Special Fellow.

1. Li, J., Yen, C., Liaw, D., Podsypanina, K., Bose, S., Wang, S. I., Puc, J., Miliaresis, C., Rodgers, L., McCombie, R., *et al*. (1997) *Science* **275**, 1943–1947.
2. Steck, P. A., Pershouse, M. A., Jasser, S. A., Yung, W. K., Lin, H., Ligon, A. H., Langford, L. A., Baumgard, M. L., Hattier, T., Davis, T., *et al.* (1997) *Nat. Genet.* **15,** 356–362 .
3. Li, D. M. & Sun, H. (1997) *Cancer Res.* **57,** 2124–2129.
4. Wang, S. I., Puc, J., Li, J., Bruce, J. N., Cairns, P., Sidransky, D. & Parsons, R. (1997) *Cancer Res.* **57,** 4183–4186.
5. Wang, S. I., Parsons, R. & Ittmann, M. (1998) *Clin. Cancer Res.* **4,** 811–815.
6. Teng, D. H., Hu, R., Lin, H., Davis, T., Iliev, D., Frye, C., Swedlund, B., Hansen, K. L., Vinson, V. L., Gumpper, K. L., *et al.* (1997) *Cancer Res.* **57,** 5221–5225.
7. Tashiro, H., Blazes, M. S., Wu, R., Cho, K. R., Bose, S., Wang, S. I., Li, J., Parsons, R. & Ellenson, L. H. (1997) *Cancer Res.* **57,** 3935–3940.
8. Risinger, J. L., Hayes, A. K., Berchuck, A. & Barrett, J. C. (1997) *Cancer Res.* **57,** 4736–4738.
9. Kong, D., Suzuki, A., Zou, T. T., Sakurada, A., Kemp, L. W., Wakatsuki, S., Yokoyama, T., Yamakawa, H., Furukawa, T., Sato, M., *et al*. (1997) *Nat. Genet.* **17,** 143–144.
10. Cairns, P., Okami, K., Halachmi, S., Halachmi, N., Esteller, M., Herman, J. G., Jen, J., Isaacs, W. B., Bova, G. S. & Sidransky, D. (1997) *Cancer Res.* **57,** 4997–5000.
11. Guldberg, P., thor Straten, P., Birck, A., Ahrenkiel, V., Kirkin, A. F. & Zeuthen, J. (1997) *Cancer Res.* **57,** 3660–3663.
12. Rhei, E., Kang, L., Bogomolniy, F., Federici, M. G., Borgen, P. I. & Boyd, J. (1997) *Cancer Res.* **57,** 3657-3659.
13. Bose, S., Wang, S. I., Terry, M. B., Hibshoosh, H. & Parsons, R. (1998) *Oncogene* **17**, 123–127.
14. Rasheed, B. K., Stenzel, T. T., McLendon, R. E., Parsons, R., Friedman, A. H., Friedman, H. S., Bigner, D. D. & Bigner, S. H. (1997) *Cancer Res.* **57,** 4187–4190.
15. Liaw, D., Marsh, D. J., Li, J., Dahia, P. L., Wang, S. I., Zheng, Z., Bose, S., Call, K. M., Tsou, H. C., Peacocke, M., *et al. (1997) Nat. Genet.* **16,** 64–67.
16. Marsh, D. J., Coulon, V., Lunetta, K. L., Rocca-Serra, P., Dahia, P. L., Zheng, Z., Liaw, D., Caron, S., Duboue, B., Lin, A. Y., *et al*. (1998) *Hum. Mol. Genet.* **7,** 507–515.
17. Carlson G. J., Nivatvongs, S. & Snover, D. C. (1984) *Am. J. Surg. Pathol.* **8,** 763–770.
18. Kay, P. S., Soetikno, R. M., Mindelzun, R. & Young, H. S. (1997) *Am. J. Gastroenterol.* **92,** 1038–1040.
19. Marsh, D. J., Dahia, P. L., Zheng, Z., Liaw, D., Parsons, R., Gorlin, R. J. & Eng, C. (1997) *Nat. Genet.* **16,** 333–334.
20. Arch, E. M., Goodman, B. K., Van Wesep, R. A., Liaw, D., Clarke, K., Parsons, R., McKusick, V. A. & Geraghty, M. T. (1997) *Am. J. Med. Genet.* **71,** 489–493.
21. Furnari, F. B., Lin, H., Huang, H. S. & Cavenee, W. K. (1997) *Proc. Natl. Acad. Sci. USA* **94,** 12479–12484.
22. Li, J., Simpson, L., Takahashi, M., Miliaresis, C., Myers, M. P., Tonks, N. & Parsons, R. (1998) *Cancer Res.* **58,** 5667–5672.
23. Maehama, T. & Dixon, J. E. (1998) *J. Biol. Chem.* **273,** 13375–13378.
24. Myers, M. P., Pass, I., Batty, I. H., Van der Kaay, J., Stolarov, J. P., Hemmings, B. A., Wigler, M. H., Downes, C. P. & Tonks, N. K. (1998) *Proc. Natl. Acad. Sci. USA* **95,** 13513–13518.
25. Stambolic, V., Suzuki, A., de la Pompa, J. L., Brothers, G. M., Mirtsos, C., Sasaki, T., Ruland, J., Penninger, J. M., Siderovski, D. P. & Mak, T. W. (1998) *Cell* **95,** 29–39.
26. Haas-Kogan, D., Shalev, N., Wong, M., Mills, G., Yount, G. & Stokoe, D. (1998) *Curr. Biol.* **8,** 1195–1198.
27. Zeitlin, S., Liu, J. P., Chapman, D. L., Papaioannou, V. E. & Efstratiadis, A. (1995) *Nat. Genet.* **11,** 155–163.
28. Cattoretti, G., Becker, M. H., Key, G., Duchrow, M., Schluter, C., Galle, J. & Gerdes, J. (1992) *J. Pathol.* **168,** 357–363.
29. Ye, B. H., Cattoretti, G., Shen, Q., Zhang, J., Hawe, N., de Waard, R., Leung, C., Nouri-Shirazi, M., Orazi, A., Chaganti, R. S. K., *et al*. (1997) *Nat. Genet.* **16,** 161–170.
30. Secord, E. A., Edington, J. M. & Thorbecke, G. J. (1995) *Am. J. Pathol.* **147,** 422–433.
31. Wells, S. M., Kantor, A. B. & Stall, A. M. (1994) *J. Immunol.* **153,** 5503–5515.
32. Hansen, G. M. & Justice, M. J. (1998) *Mamm. Genome* **9,** 88–90.
33. Adachi, M., Suematsu, S., Kondo, T., Ogasawara, J., Tanaka, T., Yoshida, N. & Nagata, S. (1995) *Nat. Genet.* **11,** 294–300.
34. Su, L. K., Kinzler, K. W., Vogelstein, B., Preisinger, A. C., Moser, A. R., Luongo, C., Gould, K. A. & Dove, W. F. (1992) *Science* **256,** 668–670.
35. Zhu, Y., Richardson, J. A., Parada, L. F. & Graff, J. M. (1998) *Cell* **94,** 703–714.
36. Griebel, P. J. & Hein, W. R. (1996) *Immunol. Today* **17,** 30–39 (1996).
37. Kerneis, S., Bogdanova, A., Kraehenbuhl, J. P. & Pringault, E. (1997) *Science* **277,** 949–952.
38. Kinzler, K. W. & Vogelstein, B. (1998) *Science* **280**, 1036–1037.
39. Di Cristofano, A., Pesce, B., Cordon-Cardo, C. & Pandolfi, P. P. (1998) *Nat. Genet.* **19,** 348–355.
40. Suzuki, A., de la Pompa, J. L., Stambolic, V., Elia, A. J., Sasaki, T., Barrantes, I. B., Ho, A., Wakeham, A., ltie, A., Khoo, W., *et al.* (1998) *Curr. Biol.* **8,** 1169–1178.